INTERNATIONAL JOURNAL OF INTEGRATED ENGINEERING
ISSN: 2229-838X e-ISSN: 2600-7916

IJIE

Vol. 17 No. 9 (2025) 393-408
https://publisher.uthm.edu.my/ojs/index.php/ijie

Raw Hard Clam as Adsorbent to Remove Phosphate in Water: Removal Prediction, Kinetic and Isotherm Model Study

Norzainariah Abu Hassan[1]*, Sheikh Muhammad Fadhlullah Baktal Sheikh Farhan Bakatal[2], Muhammad Sharif Mohamed Mubarak Ali[2], Yasmin Raihana Ramle[2], Nur Husna Muslim[1], Noorul Hudai Abdullah[2]*, Radin Maya Saphira Radin Mohamed[3], Nur Atikah Abdul Salim[4]

[1] *Faculty of Engineering Technology, Universiti Tun Hussein Onn Malaysia, Hab Pendidikan Tinggi Pagoh, Km 1, Jalan Panchor, 84600 Muar, Johor, MALAYSIA*
[2] *Neo Environmental Technology, Centre for Diploma Studies, Universiti Tun Hussein Onn Malaysia, Pagoh Education Hub, 84600 Pagoh, Johor, MALAYSIA*
[3] *Faculty of Civil Engineering and Built Environment, Universiti Tun Hussein Onn Malaysia, Batu Pahat, Johor 86400, MALAYSIA*
[4] *School of Occupational, Safety & Health, Netherlands Maritime University College, Johor Bahru, Johor, 80000 MALAYSIA*

*Corresponding Author: norzainariah@polimelaka.edu.my
DOI: https://doi.org/10.30880/ijie.2025.17.09.027

Article Info

Received: 31 January 2025
Accepted: 29 September 2025
Available online: 31 December 2025

Keywords

Raw hard clam shell, phosphorus, kinetic, isotherm, prediction

Abstract

Phosphorus pollution from various sources like agriculture, untreated industry, and domestic wastewater is a significant cause of water contamination. It can trigger eutrophication, marked by an excessive supply of nutrients that fuel the rapid growth of algae and aquatic plants. This, in turn, can lead to harmful algal blooms, severely reducing oxygen levels in the water and affecting marine life, including fish and other creatures suffering from the lack of oxygen. The purpose of this study is to evaluate how effectively raw hard clam shells remove phosphate from synthetic wastewater through batch experimental testing. Batch experiments were conducted using raw hard clam shells (particle sizes 1.18 to 2.36 mm) mixed in an orbital shaker at 170 rpm using potassium dihydrogen phosphate solution, 100 mL at a particular time, until an equilibrium state. The batch experiment data evaluating phosphate removal from raw hard clam shells had the highest removal effectiveness of 99.6%. The kinetic study proves that the predominant adsorption mechanism between the adsorbent and adsorbate involves chemisorption, where electron sharing occurs, forming chemical bonds. The adsorption isotherm data showed suitability for the Langmuir model, indicating that adsorption happens at particular binding sites in monolayer adsorption on the adsorbent surface. Additionally, the data can be used to understand the prediction contour of mass of adsorbent required and removal efficiency under various beginning concentrations from research using batch experiments. The significant potential of this study is that the Raw Hard Clam Shells adsorbent is a sustainable and eco-friendly material for tackling phosphate pollution in future wastewater treatment.

1. Introduction

The uncontrolled wastewater discharge into the environment, which results from increasing demands from an expanding population and industrial activity, seriously threatens ecosystems and public health [1]. This discharge contaminates land, streams, and marine environments with a concoction of hazardous chemicals, heavy metals, and organic contaminants [2]. The repercussions are severe, endangering the health of people and wildlife and upsetting the aquatic ecosystems. In freshwater bodies, phosphorus is thought to be the primary factor contributing to water pollution. The widespread distribution of phosphorus into the environment, originating from various sources such as agricultural runoff, industrial emissions, and wastewater, is a primary contributor to water pollution. This phosphorus influx enters rivers, lakes, and oceans [3]. The surplus phosphorus within water systems can initiate a phenomenon known as eutrophication. Poyang Lake in China is an example of a river that has experienced severe eutrophication [4] and has been studied by researchers from China. This process involves an overabundance of nutrients that stimulate the rapid proliferation of algae and aquatic plants, eventually leading to detrimental algal blooms and ultimately causing a depletion of oxygen levels within the water. As a result, these oxygen-deprived conditions adversely affect aquatic life, including fish and other organisms. High nutrient levels in water bodies are mainly caused by human activities, where excessive nitrogen and phosphorus are the leading causes of this issue.

The amount of specific dangerous substances that can be discharged into the environment by domestic and industrial wastewater treatment is regulated by effluent standards. Effluent standards for phosphorus in Europe and Malaysia are different. In Europe, the rules are strict, focusing on keeping water clean and preventing issues like eutrophication. The effluent standard of Europe is 1.0-2.0 mg/L [5]. In Malaysia, the standards can be more flexible and vary based on the facility, type of discharge, and local environmental goals. The effluent standard of Malaysia is 5 mg/L at standard A and 10 mg/L at standard B (Section 3 Sewage Characteristics and Effluent Discharge Requirements, 2009). The effluent standards in the United Kingdom are more stringent than those in Malaysia.

Wastewater treatment is essential to protecting the environment because it counteracts these negative consequences [6]. Wastewater treatment plants use chemical, biological and physical techniques to remove or neutralise pollutants before release to protect downstream ecosystems and water quality. Phosphate can be successfully removed from wastewater using various techniques, each with unique benefits and uses. One popular method that involves adding chemicals to sewage, such as ferric chloride or aluminium sulfate (alum), is chemical precipitation. By reacting with phosphate ions, these substances create insoluble precipitates that can be filtered or settled to remove from the water. Conversely, biological phosphorus removal uses the activities of microorganisms found in activated sludge systems, known as organisms, that accumulate phosphorus (PAOs) [7]. These microorganisms absorb phosphate from wastewater and store it in their cells when operating in an anaerobic environment. The phosphate that has been held is released when exposed to aerobic conditions, making it possible to remove it later by settling or filtering. Another practical approach is adsorption, which uses substances like metal oxides, activated charcoal, or zeolites with a strong affinity for phosphate ions [3]. Phosphate ions are adsorbed onto the surface of an adsorbent material bed after wastewater passes over it. This method provides effective phosphate removal and can be especially helpful when phosphate from wastewater streams needs to be continuously or selectively removed.

Conventional wastewater treatment processes rely heavily on chemicals like zeolite and activated alumina to remove phosphorus from wastewater. While these chemicals effectively reduce phosphorus levels, they pose a significant environmental risk. The disposal of chemical-laden wastewater and the production of these chemicals contribute to environmental pollution and resource depletion. This highlights the need for an approach to phosphorus removal in water treatment that is both more sustainable and environmentally friendly. Accepting natural resources as adsorbents, such as unprocessed hard clam shells, offers a viable way forward and a sustainable substitute for artificial chemicals. These organic materials can function as efficient adsorbents, eliminating contaminants such as phosphorus from wastewater and lowering the need for potentially dangerous chemicals. Disposable hard clam shells, a byproduct of various industries, are frequently disposed of inappropriately, either into the seaside or landfills. This careless disposal practice has far-reaching consequences, including the alteration of soil composition, contamination of waterways, and disturbance of marine habitats. The accumulation of clam shells results in an aesthetic nuisance, which further disturbs the ecological balance of the environment. Several initiatives have been proposed to manage shell waste, ranging from small-scale uses in decorative products to more scientifically relevant applications, such as its utilization as an adsorbent in water treatment. A mussel shell is a seashell that has been studied and researched. As a result, the shells can adsorb 90% of phosphorus from wastewater [8].

Nowadays, adsorption is one of the methods used for water treatment, such as removing phosphorus [9]. Many researchers have directed their attention toward using adsorption techniques for water treatment. Numerous innovations and advancements have emerged within this field, primarily emphasizing cost reduction and substituting conventional materials with eco-friendly alternatives. Materials such as mussel shells [10],

eggshells [11], red mud [12], clay-oyster shells [13], and zeolite [14] have been used to remove phosphorus from wastewater. This study has changed the material to be more environmentally friendly, a hard clam shell. The hard clamshell contains a similar composition to the mussel shell, which is calcium carbonate [15]. Although various materials studies are applied on adsorption to remove pollutants in water, the prediction of phosphorus removal, kinetic, and isotherm modeling studies needs to be verified due to limited investigation on raw hard clam shell species in Malaysia. In specific, the objectives are as follows: (1) to determine the effectiveness of phosphorus removal through Raw Hard Clam Shells as adsorbents and analyze the adsorption capacity until the equilibrium state, (2) to evaluate the prediction contour of removal efficiency and mass of adsorbent needed under different initial concentrations from batch experiment studies, and (3) to investigate the theoretical and batch experimental data using kinetic (Pseudo-First Order and Pseudo-Second-Order) and isotherm (Langmuir and Kinetic) modeling studies.

2. Materials and Methods

2.1 Preparation and Characterization of Adsorbent

In this study, discarded hard clam shells were employed as an absorbent. The hard clam shells were obtained at Bachok, Kelantan. The shells were first rinsed with purified water to remove impurities, followed by a drying process at 30°C in an oven for two days [16]. After two days, the shells were ground and sieved into particle sizes of 1.18–2.36 mm. Lastly, the prepared powder or adsorbent was weighed and packed into 2, 4, 6, 8, and 10 g for batch experiment. Physical-chemical traits denote the attributes of substances that can be observed in the different characteristics before and after adsorption. This study involved several analyses, including XRD analysis (X-ray diffraction) performed to observe the crystalline structure of raw hard clam shells, conducted at Makmal Fizik Bahan, Kampus Pagoh, UTHM. The XRD patterns display specific diffraction peaks, providing insights into the crystalline phases existing in the material. Energy Dispersive X-Ray Fluorescence (EDXRF) analysis tested using EM-30AX Plus at Makmal Fizik Teknologi Nano, Kampus Pagoh, UTHM, to determine the elemental composition of the raw hard clam shell. The results indicate the presence of various elements, including calcium, carbon, oxygen, and traces of other elements. Scanning Electron Microscopy (SEM) was conducted using EM-30AX Plus at Makmal Fizik Teknologi Nano, Kampus Pagoh, UTHM to explore the surface morphology and porosity of raw white hard clam shell. The SEM images revealed a complex and porous surface structure. Fourier Transform Infrared Spectroscopy (FTIR) was utilised using Perkin Elmer Spectrum Two FTIR Spectrometer at Food Instrumentation Centre Lab, Kampus Pagoh, UTHM, to characterize the functional groups and chemical bonding found in the raw hard clam shell.

2.2 Preparation of Aqueous Solution Phosphate and Testing

The aqueous phosphate synthetic solution containing 100 mg/L of PO_4^{3-} was prepared by dissolving 0.1433 g of potassium dihydrogen phosphate (KH_2PO_4) in one liter of deionized water using a volumetric flask [8]. Then, deionized water was used to dilute the synthetic solution into 50, 25, 20, 15, 10, and 5 mg/L, respectively [17]. The dilution of the desired initial solution volume was calculated using equation (1).

$$C_1V_1 = C_2V_2 \quad (1)$$

where C_1 is concentration 1 with volume 1 (V_1), and C_2 is concentration 2 with volume 2 (V_2), respectively. Phosphorus levels were measured using the HACH DR 6000 UV-Vis, applying the amino acid method 490 specifically tailored for phosphate determination. All analytical techniques for various parameters will comply with the protocols detailed in the Standard Methods for the Examination of Water and Wastewater ensuring the utilization of established and acknowledged methodologies throughout the testing and analysis procedures.

2.3 Batch Experiment

The synthetic phosphate solution used in the adsorption kinetic and isotherm tests contained 10 mg/L of PO43. Erlenmeyer flasks with different adsorbent mass (2 g, 4 g, 6 g, 8 g, and 10 g) were filled with 100 mL of the phosphate solution for the batch experiment. These flasks were shaken constantly for 30, 90, 150, 270, 300, and 4320 minutes at 170 rpm. This study aimed to examine the removal efficiency and adsorption capacity of phosphate onto hard clam shell under different conditions to provide light on the dynamic behaviour of the adsorption process across different contact times and adsorbent masses. As indicated in Fig. 3, the mixes were shaken at 170 rpm to investigate the adsorption equilibrium between the phosphate and adsorbent at various masses and contact times. The adsorbents were taken out of the flask, filtered, and analysed. The phosphate content was determined using the Amino Acid Method and the HACH DR6000 UV-Spectrophotometer [18].

Equations (2) and (3) were applied to determine the adsorption capacity (q) and removal efficiency (E), respectively. The formulas for the adsorption capacity and removal efficiency [19] is expressed as,

$$q = \frac{(C_i - C_f) \times V}{m} \quad (2)$$

The adsorption capacity (q) in the equations is expressed in mg/g, the initial phosphate concentration (C_i) in mg/L, the phosphate concentration in the solution (C_f) as mg/L, the mass of the adsorbent (m) as g, as well as the solution's quantity (L) as V.

$$E = \frac{(C_i - C_f)}{C_i} \times 100\% \quad (3)$$

Here, C_i is the starting phosphate concentration (mg/L), E entails the elimination effectiveness (%), and C_f is the phosphate concentration in the solution (mg/L).

2.4 Kinetic, Isotherms Studies, and Prediction Contour Analysis

Kinetic studies observe how quickly a chemical reaction advances with time, whereas isotherm studies analyse how a substance behaves in adsorption under varying concentrations and temperatures. For the kinetic model, Pseudo-First Order and Pseudo-Second-Order were used. Pseudo-first order is important for investigating adsorption processes, especially in comprehending the rate of phosphate removal when using raw hard clam shells as an adsorbent. While pseudo-second order is a helpful method for studying how substances stick to surfaces, it is beneficial for figuring out how quickly phosphate is removed when using raw hard clam shells. This study explored both the Freundlich and Langmuir models for isotherm model studies. According to the Langmuir model, adsorption occurs in a monolayer with maximum surface occupancy, with the molecules adsorbed as a single layer rather than forming multiple layers. However, this finding does not mean that the Freundlich isotherm is limited. The Freundlich adsorption isotherm is applied to evaluate how the amount of solution adsorbed by a unit mass of adsorbents changes as system pressure varies at a given temperature. To evaluate the adequacy and accuracy of the adsorption isotherm and kinetic models, several error functions (F_e) were applied, including the coefficient of determination (R^2). These functions were selected because they provide robust indicators of model performance, measuring the closeness of predicted values to experimental data. In this study, Microsoft Excel was used to generate contour prediction plots, which helped visualize how changes in adsorbent dosage and initial phosphate concentration influenced removal efficiency. Excel was chosen as it offers a simple yet effective way to capture these relationships and provide practical insights without the need for more complex modeling software.

3. Results and Discussion

3.1 Characteristics of Samples

The surface morphology of the raw hard clam shell was investigated using scanning electron microscopy (SEM, model EM-30AX Plus; manufacturer: COXEM, Location: Daejeon, Korea) before and after adsorption. The scanning electron microscope (SEM) was utilized to observe the surface features at the minuscule nanoscale level [20]. Fig. 1 shows an SEM photograph of the raw hard clam shell before and after with 1000×, 2000×, and 3000× magnification. Fig. 1 (a), (b), and (c) before adsorption shows that at 1000× magnification, the sample had a compact texture and was a little brighter compared to after adsorption (Fig. 1(d), (e), and (f)), show that the darkness is more prominent. The coating on its surface might be phosphorus.

The raw hard clam shell composition was tested using energy-dispersive X-ray fluorescence (EDXRF) and the EM-30AX Plus apparatus from COXEM in Daejeon, Korea. Major and minor elements in various algae species can be identified using EDXRF [21]. Table 3 shows the compositional aspects of Raw Hard Clam Shells before and after. The composition before is Ca (42.73%), C (10.26%), and O (47.02%). While raw hard clam shell after there is an increase in the value of P and Ca and a decrease in O and C that is, Ca (60.38), C (6.89%), P (0.29%), and O (32.41%). After undergoing the process within HCS, there is a conspicuous increase in calcium and phosphorus concentrations. This event suggests that removing phosphorus from the aqueous solution involved calcium significantly. It seems phosphorus formed bonds with calcium ions due to calcium facilitating its ionization. This suggests a complex interaction between calcium oxide and phosphorus, highlighting the significance of calcium in the process [18].

Int. Journal of Integrated Engineering Vol. 17 No. 9 (2025) p. 393-408

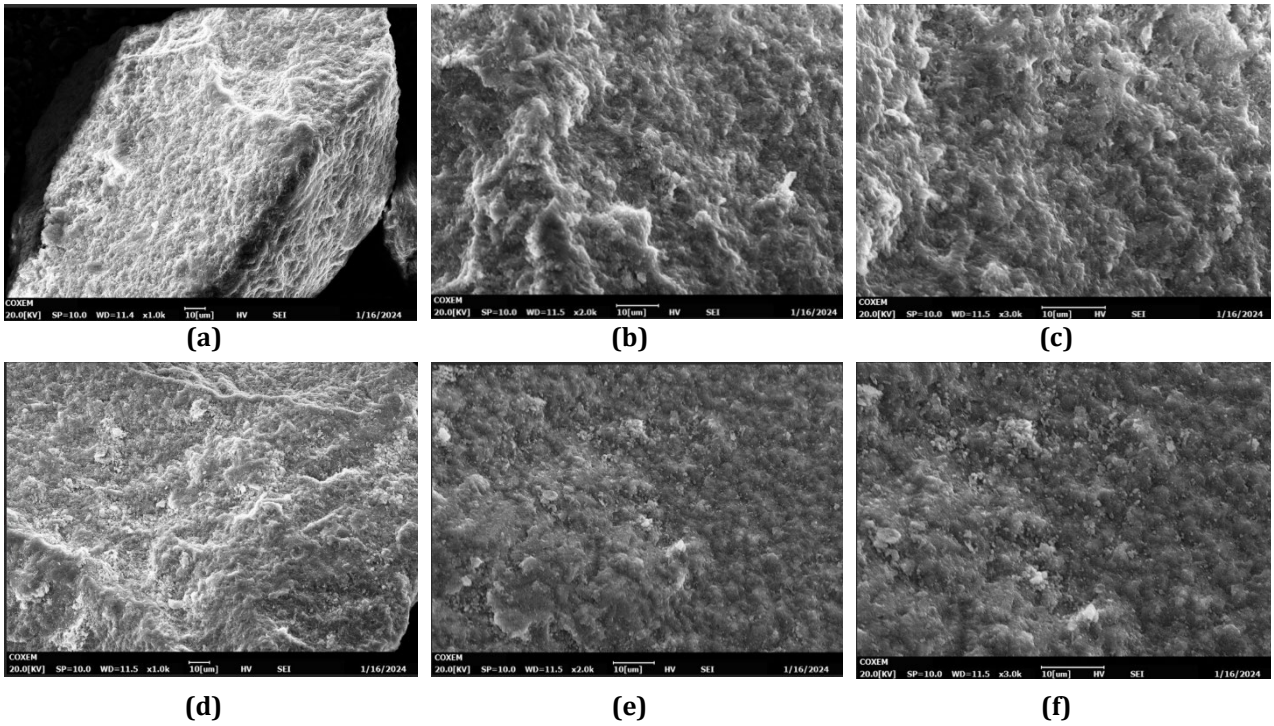

Fig. 1 *SEM images of raw hard clam shell before adsorption (a) 1000×; (b) 2000×; (c) 3000× magnification ratios. After adsorption, (d) 1000×; (e) 2000×; (f) 3000× magnification ratios*

Table 1 *Composition of the raw hard clam shell (wt. %) by EDXRF*

Element	Calcium	Carbon	Phosphorus	Oxygen	Total
Before (%)	42.73	10.26	0.00	47.02	100
After (%)	60.38	6.89	0.29	32.4	100

With the Perkin Elmer Spectrum Two FTIR Spectrometer (United States), Fourier Transform Infrared (FTIR) Spectroscopy, one may characterise the functional groups in the raw hard clam shell before and after the adsorption (see Table 1). Other than that, FTIR spectrometer was employed to gather sample data across the entire detection range, and initial data were adjusted for spectral baseline drift to facilitate quantitative analysis [22]. Fig. 2(a) describes the FTIR peak value of raw hard clam shell in 1.18–2.36 mm, representing the CaCO3 peak value before adsorption. The FTIR spectrum depicted in Fig. 2 compares the original state of the raw hard shell with the state with adsorbedPO_4^{3-} ions, covering the range of 700–4000 cm^{-1}. This analysis aims to distinguish changes in surface functional groups.

Table 2 provides a detailed breakdown of the FTIR spectrum before and after PO_4^{3-} adsorption. The nature and arrangement of these surface functional groups play an essential role in shaping the PO_4^{3-} stretching band observed in the raw hard clam shell FTIR spectrum. The functional group at 701 cm^{-1} and 704 cm^{-1} before and after PO_4^{3-} adsorption with a 3 cm^{-1} difference indicates the aromatic group. The 850 cm^{-1} and 898 cm^{-1} peaks represent the aliphatic functional group that remains consistent before and after adsorption. There is also a single value without a pair at 1077 cm^{-1} and 2240 cm^{-1} before the adsorption, which indicates the phenolic acid and carbon-deuterium, respectively, and at 1994 cm^{-1} and 2527 cm^{-1} , which are classified as alkane and Thiol. For peak values that exceed 3000 cm^{-1} , many do not have a partner. Before adsorption, peak values 3496 cm^{-1} and 847 cm-1 are in the hydroxyl functional group. The lone peak values without a corresponding pair are 3183 cm-1 (chitosan), 3340 cm-1 (hydroxyl), 3597 cm-1, and 3735 cm-1 (both representing amino groups).

Various peaks within 1400–3100 cm^{-1} reveal specific functional groups. Peaks at 1450–1454 cm^{-1} and 1644-1 654 cm^{-1} signify the presence of carboxylate groups. Additionally, a peak around 1778–1782 cm^{-1} suggests the presence of carboline, while 2233 cm^{-1} indicates the carbon-deuterium functional group, consistent before and after adsorption. Further, the nitrile and thiol functional groups are evident at 2292–2296 cm^{-1} and 2505–2508 cm^{-1} , respectively. Notably, a consistent peak at 2632 cm^{-1} and 2755 cm^{-1} represents hydroxyl groups before and after adsorption. Moreover, methyl groups appear at 2937 cm^{-1} , alkenes at 3034 cm^{-1} , and chitosan at 3116 cm^{-1}. Based on the analyses of Fig. 2(a) and (b), it was determined that minimal alterations were observed before and after the adsorption process. While there was a discernible change in the peak value, the functional group exhibited consistency in its range for Fig. 2(a) and (b).

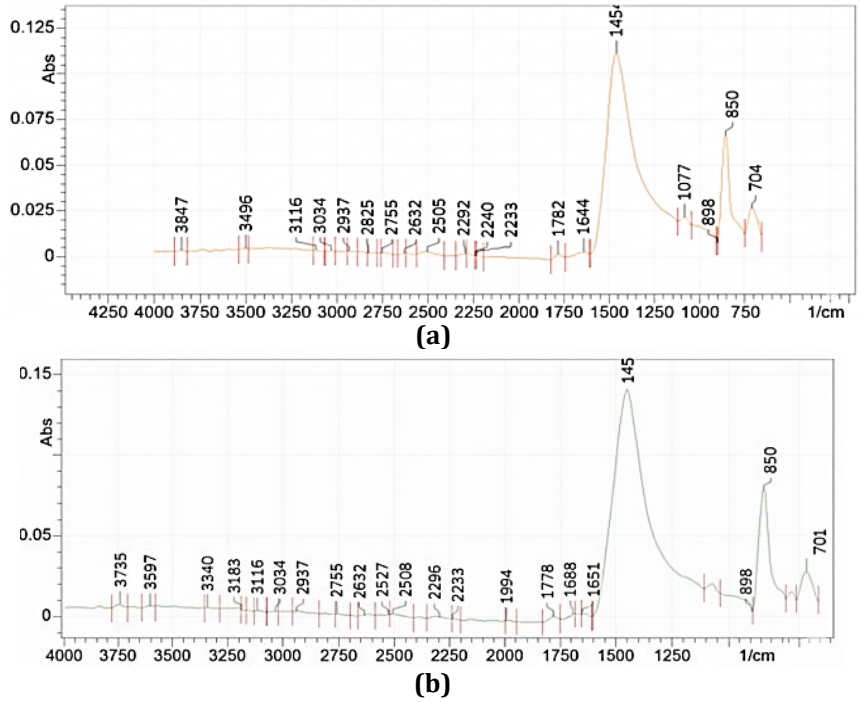

Fig. 2 *FTIR peak value for raw hard clam shell (a) Before the adsorption process; (b) After the adsorption process*

Table 2 *Functional group by the peak value for before and after adsorption by FTIR analyses*

Before (cm^{-1})	After (cm^{-1})	Functional Group	Reference
704	701	Aromatics	[23]
850	850	Aliphatic	[23]
898	898	Aliphatic	[23]
1077	-	Acid Phenol	[24]
1454	1450	Carboxylate	[25]
1644	1651	Carboxylate	[26]
1782	1778	Carbolyn	[27]
-	1994	Alkane	[28]
2233	2233	Carbon-deuterium	[27]
2240	-	Carbon-deuterium	[27]
2292	2296	Nitrile	[29]
2505	2508	Thiol	[28]
-	2527	Thiol	[28]
2632	2632	Hydroxyl	[28]
2755	2755	Hydroxyl	[28]
2937	2937	Methyl	[24]
3034	3034	Alkenes	[30]
3116	3116	Chitosan	[30]
-	3183	Chitosan	[30]
-	3340	Hydroxyl	[31]
3496	-	Hydroxyl	[31]
-	3597	Amino	[32]
-	3735	Amino	[32]
3847	-	Hydroxyl	[33]

Int. Journal of Integrated Engineering Vol. 17 No. 9 (2025) p. 393-408

The crystallisation or phase composition of raw hard clam shell can be analysed using the Second-generation BRUKER D2 Phaser Benchtop X-ray Diffractometer (XRD). Furthermore, XRD analysis enabled a precise crystallite size estimation, aiding in the customisation for enhanced photocatalytic activity [34]. Fig. 3(a) describes the XRD peak value of raw hard clam shell in 1.18 mm–2.36 mm, representing the crystal phase composition in the pie chart and the peak value of raw hard clam shell before the process adsorption. As shown in the pie chart Fig. 3(a), the predominant components were gamma oxygen (64%) and lime (36%), commonly recognised as calcium hydroxide. In contrast, in pie chart Fig.3(b), the major constituents were eta oxygen (61%) and calcium oxide (39%). The contrast between the two pie charts shows how a raw hard clam shell changes when it interacts with phosphorus. This suggests it could be helpful in removing phosphorus from water. The switch from calcium hydroxide to calcium oxide indicates a significant change in the material's structure caused by phosphorus [35]. Also, the primary oxygen type change hints at a surface change, likely due to phosphorus interacting with it.

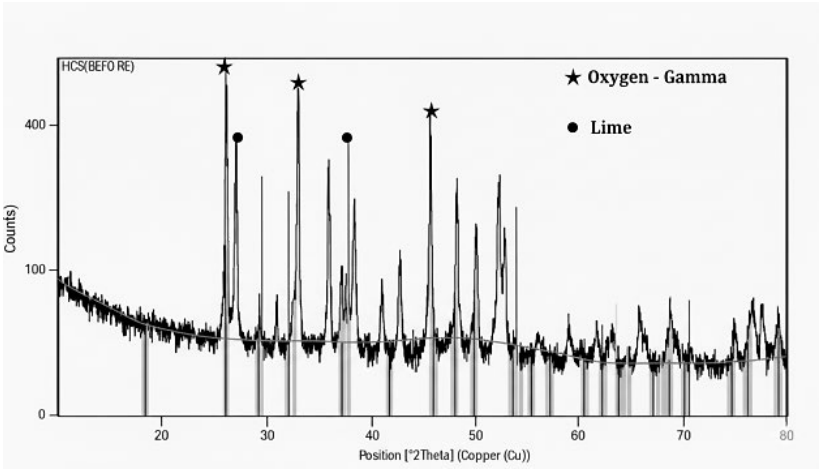

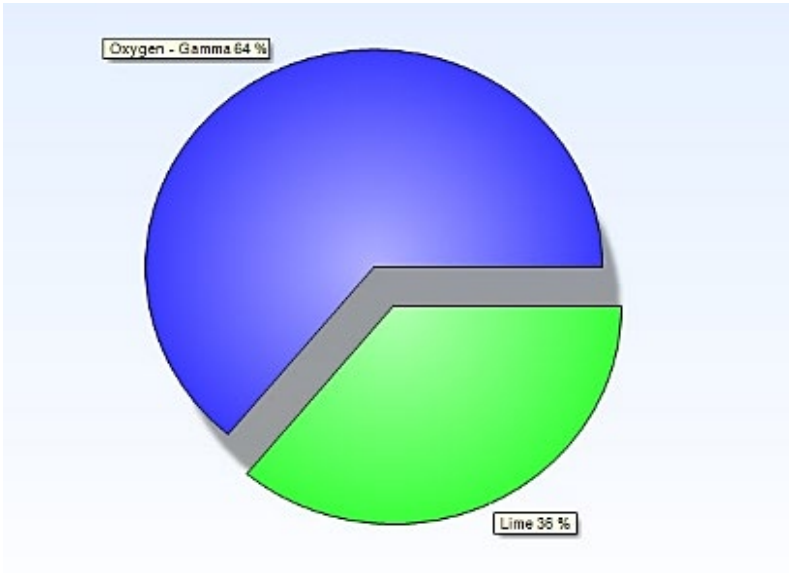

(a)

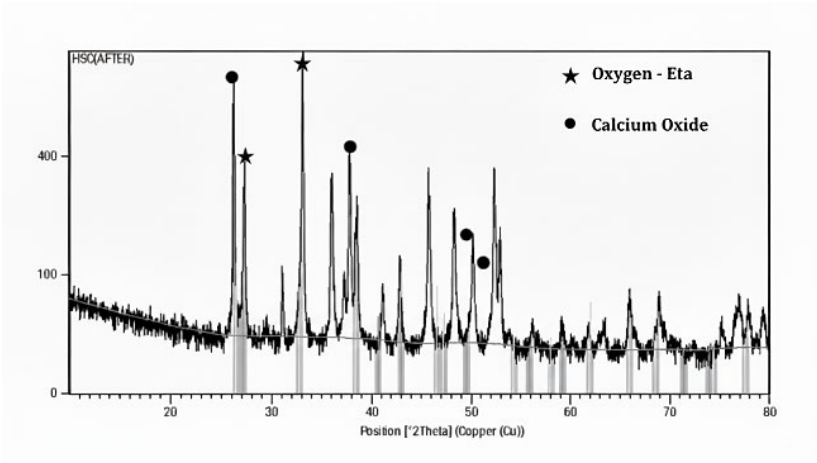

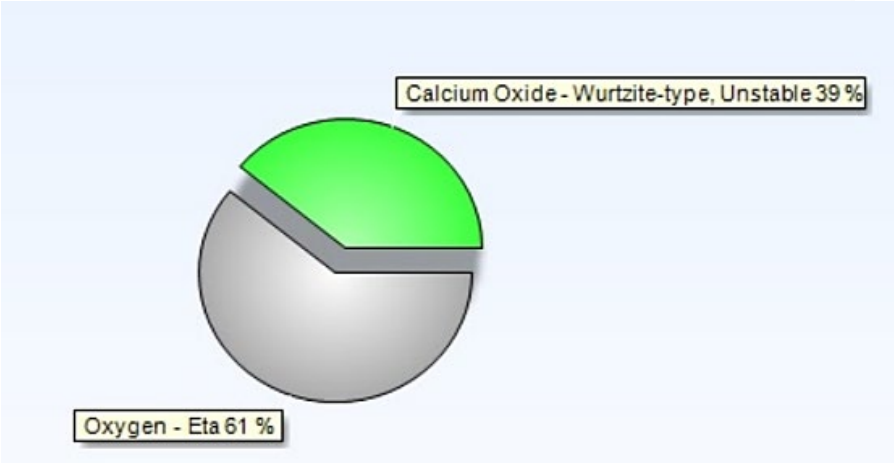

(b)

Fig. 3 *XRD peak value and pie chart for raw hard clam shell (a) Before the adsorption process; (b) After the adsorption process*

3.2 Adsorption of Phosphorus

At 4320 minutes of contact time, the phosphate removal efficiencies (E) for raw hard clam shell dosages of 2, 4, 6, 8, and 10 g were all recorded as 100%, as depicted in Fig. 4. The calcium oxide groups on the raw hard clam shell surface have a strong attraction for phosphate ions because of their opposing charges, which is primarily responsible for the adsorption process. This creates a strong, attractive force between these components [22].

The efficiency of phosphate removal by raw hard clam shell experiences a rapid increase within the first 30 minutes of contact time for raw hard clam shell dosages of 6, 8, and 10 g, respectively. Subsequently, it continues to rise sharply until reaching a state of equilibrium. Meanwhile, dosages 2 and 4 g reached equilibrium at 90 minutes for raw hard clam shell. Hence, equilibrium times of 30 minutes were observed for phosphate adsorption onto raw hard clam shells at 6, 8, and 10 g, respectively, while a duration of 90 minutes was required for raw hard clam shells at 2 and 4 g. One explanation for the quick increase in phosphate adsorption onto raw hard clam shells from a synthetic solution could be the adsorbent surface's abundance of active sites. Phosphate from an aqueous solution has been observed to adsorb onto hard clam shells with high adsorption yields [18].

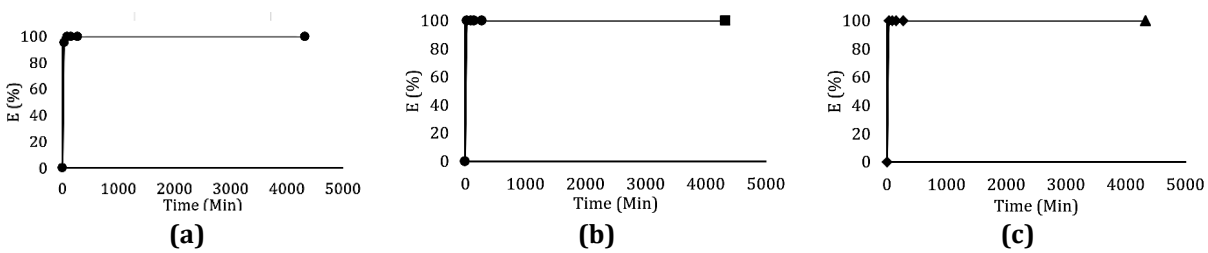

(a) **(b)** **(c)**

Int. Journal of Integrated Engineering Vol. 17 No. 9 (2025) p. 393-408

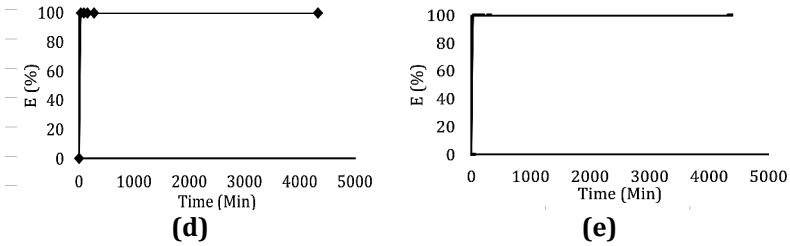

Fig. 4 *The variability in removal effectiveness of phosphate adsorption onto raw hard clam shell at (a) 2g; (b) 4g; (c) 6g; (d) 8g; (e) 10g*

For phosphate adsorption, observations were conducted on the effects of different raw hard clam shell (mass of adsorbent) concentrations on E and q using 2, 4, 6, 8, and 10 g of raw hard clam shell, as shown in Fig. 5. As raw hard clam shell levels grow from 2 to 10 g, according to Fig. 5, E for phosphate adsorption increases between 99.8% and 99.9%, whereas q_e falls from 0.6 to 0.05 mg/g. The elevated amount of raw hard clam shell is responsible for the rise in E, and it could lead to an increase in the number of active sites and surface area available for phosphate adsorption from a synthetic solution. The unsaturated adsorption active sites that remain after the adsorption process are responsible for decreased q value as the amount of raw hard clam shell increases. Comparable results for the phosphate adsorption onto calcined mussel shells have been reported, demonstrating that the value of E increases with the adsorbent's concentration [18]. Based on the EDXRF data before and after raw hard clam shell, calcium ions have a strong affinity for phosphate ions (PO_4^{3-}). When calcium ions are present in water or soil, they can adsorb phosphate ions onto their surfaces [36]. This study applied that raw hard clam can effectively remove phosphate in controlled synthetic water. However, real wastewater often contains various competing ions that may affect adsorption. To strengthen the practical relevance of this work, future studies should test the adsorbent under real wastewater conditions.

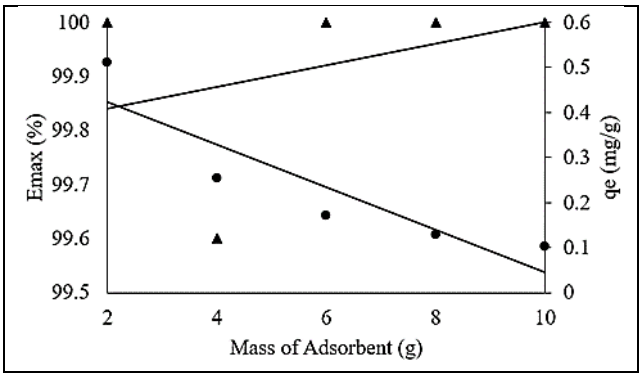

Fig. 5 *Relationship of (upper line) the removal efficiency and the amount of raw hard clam shell; (lower line) the adsorption capacity and the amount of raw hard clam shell; (upper line) E for the adsorption of phosphate and (lower line) q_e for the adsorption of phosphate*

3.3 Adsorption Kinetic

The experimental findings were employed to evaluate the adsorption kinetics of phosphate onto raw hard clam shells by applying the pseudo-first-order and pseudo-second-order equations [37]. The pseudo-first-order equation, can be stated as,

$$\ln(q_e - q_t) = \ln(q_e) - k_1 t_i \tag{4}$$

where t_i is the adsorption time (min), k_1 is a rate constant of the pseudo-first-order equation (min-1), and q_e is the equilibrium amount of phosphate adsorbed (mg/l), q_t is the quantity of phosphate adsorbed at adsorption time (mg/L). As demonstrated in Fig. 6(a), the slope and intercept of the plot of ln ($q_e - q_t$) vs t_i, respectively, can be used to determine the k1 and ln qe values. When a straight line appears on the plot of ln ($q_e - q_t$) with t_i, the adsorption kinetic is described by a pseudo-first-order model. The pseudo-second-order equation [38] is expressed as,

$$\frac{t_i}{q_t} = \frac{1}{k_2 q_e^2} + \frac{t_i}{q_e} \quad (5)$$

In the context where t_i represents the adsorption time (min), k_2 stands for the rate constant of the pseudo-second-order model (min^{-1}), and q_t (mg/g) denotes the quantity of phosphate adsorbed at a given adsorption time, q_e represents the amount of phosphate adsorbed at equilibrium (mg/g). The plot of t_i/q_t against t_i, depicted in Fig. 6(b), allows for the determination of k_2 and q_e through the intercept and slope analysis. A linear curve in the plot indicates adherence to the pseudo-second-order model for adsorption kinetics. The pseudo-first-order and pseudo-second-order models have been applied for phosphate adsorption from aqueous solutions. Table 3 provides the kinetic parameters k_1, k_2, and q_e for these two adsorption kinetic models. The F_e equation (6) is expressed as,

$$F_e = \sqrt{\left(\frac{1}{n-p}\right) \cdot \sum_i^n \left(q_{t(\exp)} - q_{t(theo)}\right)^2} \quad (6)$$

To determine the experimental quantity $q_{t(exp)}$ (mg/g), where "p" represents the number of parameters in the kinetic equation and "n" indicates the number of measurements. The choice between the pseudo-first-order and pseudo-second-order kinetic models should be made by identifying the model with the highest correlation coefficient (R^2) and the lowest F_e value. The experiments in this study were conducted without replicates; therefore, statistical measures such as standard deviation could not be reported. Instead, model adequacy was validated using error functions, namely R^2, which quantify the accuracy of model fitting. While standard deviation reflects reproducibility across repeated tests, the chosen error functions are more appropriate for assessing the reliability of the adsorption isotherm and kinetic models in this work.

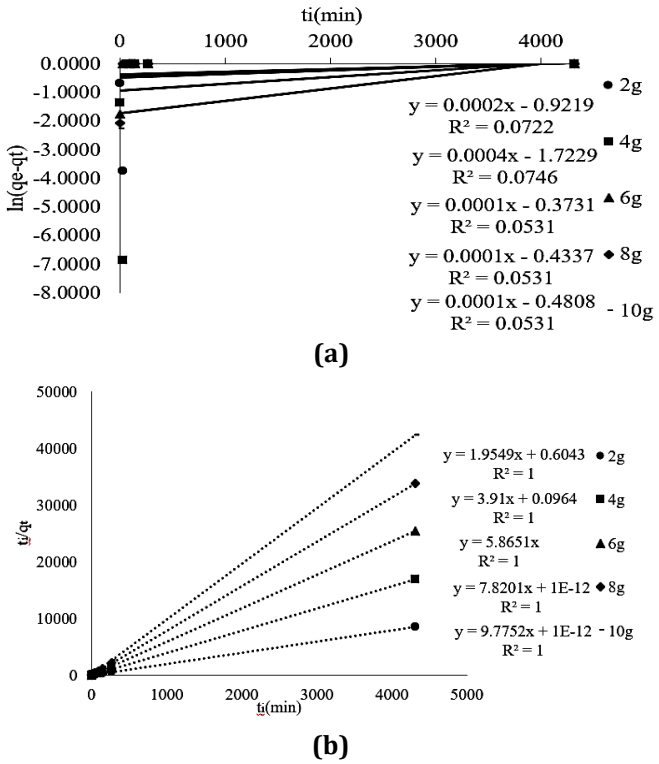

Fig. 6 *The linear regression analysis results for the phosphate adsorption onto raw hard clam shell from a synthetic solution for (a) Pseudo-first-order model; (b) Pseudo-second-order model*

Int. Journal of Integrated Engineering Vol. 17 No. 9 (2025) p. 393-408

Table 3 *The kinetic characteristics of pseudo-first- and pseudo-second-order phosphate adsorption onto raw hard clam shell*

Pseudo-First-Order					
Mass of Adsorbent (g)	$q_{(theo)}$ (mg/g)	k_1 (/Min)	R^2	F_e	$q_{(exp)}$ (mg/g)
2	0.3978	0.0002	0.0722	2.1834	0.5115
4	0.1785	0.0004	0.0746	1.0142	0.2558
6	0.6886	0.0001	0.0531	0.7836	0.1705
8	0.6481	0.0001	0.0531	0.5878	0.1279
10	0.6183	0.0001	0.0531	0.4701	0.1023
Pseudo-Second-Order					
Mass of Adsorbent (g)	$q_{(theo)}$ (mg/g)	k_2 (/Min)	R^2	F_e	$q_{(exp)}$ (mg/g)
2	0.5115	6.3241	1.0000	0.0229	0.5115
4	0.2558	158.5902	1.0000	0.0011	0.2558
6	0.1705	0.0000	1.0000	0.0000	0.1705
8	0.1279	6.1154E+13	1.0000	0.0000	0.1279
10	0.1023	9.5555E+13	1.0000	0.0000	0.1023

Table 3 demonstrates that the correlation coefficient (R^2) for the pseudo-second-order model (greater than 1.000) exceeded that (R^2> 0.722) for the pseudo-first-order model. This indicates that the pseudo-second-order kinetic model offers a more accurate depiction of the adsorption kinetics of phosphate onto raw hard clam shell from a synthetic solution compared to the pseudo-first-order model, as evidenced by the higher R^2 value and lower F_e value. These results suggest that the predominant adsorption mechanism between the adsorbent and adsorbate involves chemisorption, where electron sharing occurs, leading to the formation of chemical bonds.

3.4 Adsorption Isotherm

In this study, both the Freundlich and Langmuir models were investigated. The Langmuir model proposes the formation of a monolayer with maximum coverage, where adsorbed molecules are not arranged in layers. However, this observation does not imply that the Freundlich isotherm is restrictive. The Freundlich adsorption isotherm measures how the quantity of solution absorbed by a unit mass of solid adsorbents changes with system pressure at a constant temperature. The experimental results were evaluated using both the Langmuir and Freundlich isotherm equations. The Freundlich equation is expressed as equation (7).

$$\ln q_e = \ln K_F + \frac{1}{n} \ln C_e \tag{7}$$

where C_e is the equilibrium concentration (mg/L), n (dimensionless) is the heterogeneity factor, and q_e is the equilibrium quantity of phosphate adsorbed (mg/g). For more diverse surfaces, a lesser value is anticipated. The following represents the Langmuir equation as equation (8).

$$\frac{1}{q_e} = \frac{1}{K_L q_{max} C_e} + \frac{1}{q_{max}} \tag{8}$$

This equation is used to analyse adsorption processes, where Ce represents the equilibrium concentration (mg/ L), qe is the equilibrium adsorption quantity (mg/g), qmax stands for the maximum adsorption capacity (mg g-1), and KL denotes the adsorption energy constant (L/mg). Adsorption isotherms are valuable because they assess an adsorbent's capacity and demonstrate the relationship between this capacity and the concentration of contaminants in a liquid solution.

The Langmuir parameters K_L and q_{max} were derived from the gradient and y-intercept of the graph $1/q_e$ versus $1/C_e$, while the values of K_f and n were determined from the y-intercept and gradient of the plot $\ln(q_e)$ versus $\ln(C_e)$, as illustrated in Fig. 7. This study portrays the adsorption isotherm process through the application of the Freundlich and Langmuir models.

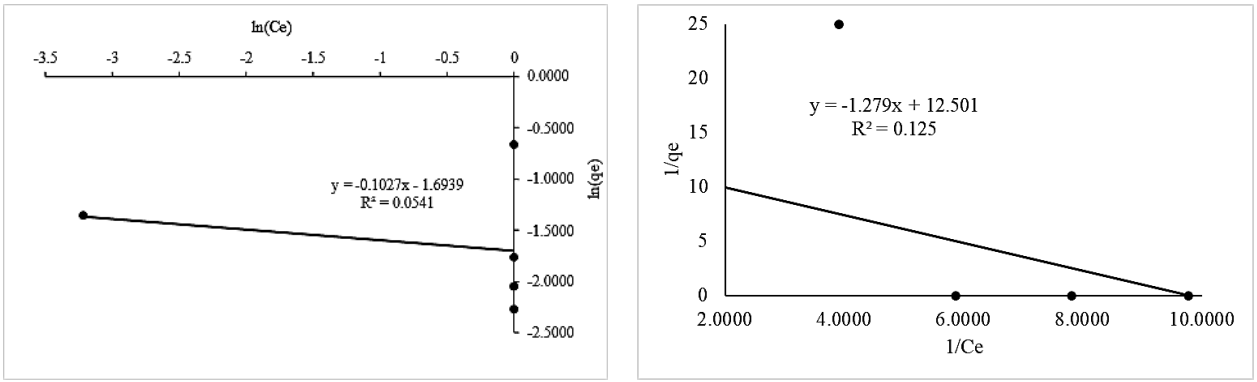

(a) **(b)**

Fig. 7 *Phosphate experiment results on HCS matched (a) Freundlich model; (b) Langmuir model*

Table 4 *The isotherm model parameter for phosphorus adsorption on raw hard clam shell*

Isotherm model	Parameter	Values
Freundlich	n	-9.7371
	K_F (mg g^{-1})	0.1838
	R^2	0.0541
Langmuir	q_{max} (mg g^{-1})	0.0799
	K_L (L mg^{-1})	-9.785
	R^2	0.1250

According to the parameters in Table 4, adsorption occurs at specific binding sites localized on the adsorbent's surface since the Langmuir model's correlation coefficient was higher than the Freundlich model. The optimal Langmuir values would indicate Langmuir isotherm constants (KL) and maximum adsorption capacities (q_{max}) that closely match the observed experimental data. In other words, the best Langmuir values would generate curves that best fit the experimental data, demonstrating that the Langmuir model accurately explains the adsorption phenomenon formation of monolayer on the adsorbent surface. This facilitates a deeper understanding of the adsorption mechanism and enables effective adsorbent utilization in environmental applications and water purification technologies.

Based on the two isotherm models, namely Freundlich and Langmuir, because the R^2 value of Langmuir is closer to one compared to Freundlich. If it is related to the SEM, XRD, and EDXRF raw, hard clam shell after, there is an additional element: the phosphorus element attached to the Raw Hard Clam Shell sample after adsorption. For example, for SEM, there is a new layer at sample Raw Hard Clam Shell after adsorption, whereas for XRD, there is oxidized calcium. For EDXRF, there is an additional element, phosphorus, in the sample raw hard clam shell after adsorption.

3.5 Removal Prediction

In this study, prediction contour was also used to analyze the effectiveness of raw hard clam shell in removing phosphorus from an aqueous solution, as shown in Fig. 8. Based on the batch experiments conducted, it was observed that the percentage of phosphorus removal increases proportionally with the increase in the weight of the raw hard clam shell sample used. According to Fig. 8, achieving complete removal (90-100%) of phosphorus from an aqueous solution containing 25 mg/L using just 8 g of raw hard clam shells is possible at point A. At point B, 6 grams of raw hard clam shells achieved 80–90% phosphorus removal from a 15 mg/L aqueous solution. Lastly, at point C, 4 grams of raw hard clam shell achieved 60-70% phosphorus removal from aqueous solutions with concentrations ranging from 10 to 15 mg/L. This indicates a direct relationship where higher weights of raw hard clam shells lead to higher percentages of phosphorus removal during adsorption.

Int. Journal of Integrated Engineering Vol. 17 No. 9 (2025) p. 393-408

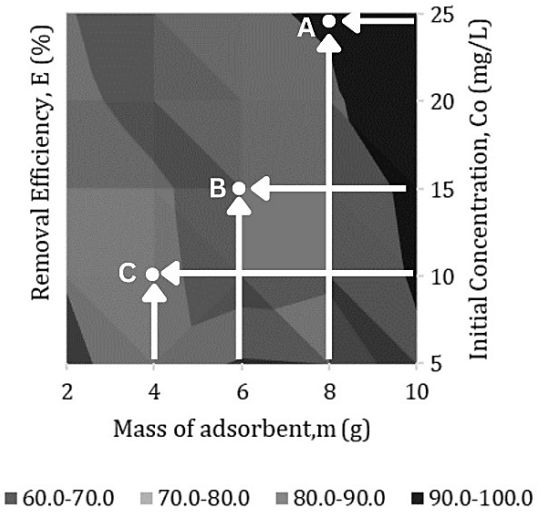

Fig. 8 *Prediction contour*

According to the prediction contour, researchers can determine the appropriate gram amount of raw hard clam shell needed for various concentrations of aqueous solutions to achieve specific percentages of phosphorus removal. These plots provide valuable insights for deeper study, offering a clearer understanding of how removal efficiency varies with initial adsorption conditions.

4. Conclusion

Since phosphate in wastewater may lead to eutrophication, it can harm the environment and negatively affect human health. Furthermore, because hard clam shells are difficult to degrade organically, their waste might contribute to pollution through exposure. This study effectively investigated the removal of phosphate from Raw Hard Clam Shells; a particle size range of 1.18 mm–2.36 mm produced the highest removal effectiveness of 99.6%. The experimental data applied the pseudo-first-order and pseudo-second-order models. With the maximum adsorption rate, the pseudo-second-order model (R^2=1.0000) performs better in capturing adsorption kinetics than the pseudo-first-order model (R^2=0.0746). These results suggest that the predominant adsorption mechanism between the adsorbent and adsorbate involves chemisorption, where electron sharing occurs, leading to the formation of chemical bonds. In addition, pseudo-second-order offers the most reliable insight into how the absorption process occurs, which can be used to optimize the absorption process in environmental remediation applications. The adsorption isotherm data showed suitability for the Langmuir model (R^2 = 0.1250), indicating that adsorption occurs at specific binding sites with monolayer adsorption on the adsorbent surface. A greater Ca concentration was found in the physicochemical analysis of hard clam shells, which is 42.73% in hard clam shells processed before and 60.38% in hard clam shells processed after. Phosphate adsorption is negatively charged and may be enhanced by a more significant positive-charged Ca concentration. The results demonstrate the potential of hard clam shells as an adsorbent for reducing phosphate in wastewater, particularly as a tertiary treatment for domestic sewage. Future studies should explore pilot-scale trials under real wastewater conditions, providing evidence that can guide industries in adopting this approach and inform policymakers in developing sustainable waste-to-resource strategies.

Acknowledgement

This research was supported by Universiti Tun Hussein Onn Malaysia (UTHM) through Tier 1 (Vot J133) and Geran Penyelidikan Pascasiswazah, GPPS (Vot Q673).

Conflict of Interest

Authors declare that there is no conflict of interests regarding the publication of the paper.

Author Contribution

The authors confirm contribution to the paper as follows: ***study conception and design:*** *Norzainariah Abu Hassan, Noorul Hudai Abdullah, Radin Maya Saphira Radin Mohamed, Nur Atikah Abdul Salim, and Nur Husna Muslim;* ***data collection, analysis and interpretation of results, and draft manuscript preparation:*** *Sheikh Muhammad Fadhlullah Baktal, Muhammad Sharif Mohamed, Yasmin Raihana Ramle. All authors reviewed the results and approved the final version of the manuscript.*

References

[1] Geueke, B., Phelps, D. W., Parkinson, L. V. & Muncke, J. (2023) Hazardous chemicals in recycled and reusable plastic food packaging, *Cambridge Prisms: Plastics*, *1,* e7, https://doi.org/10.1017/plc.2023.7

[2] Baskar, S. & Sidhaarth, K. A. (2020) Removal of nickel from water by adsorption method using clam shells, *International Journal of Advanced Research in Engineering and Technology, 11(12),* 735-749. https://doi.org/10.34218/IJARET.11.12.2020. 074

[3] Feng, L., Zhang, Q., Ji, F., Jiang, L., Liu, C., Shen, Q. & Liu, Q. (2022) Phosphate removal performances of layered double hydroxides (LDH) embedded polyvinyl alcohol/lanthanum alginate hydrogels, *Chemical Engineering Journal, 430,* 132754, https://doi.org/10.1016/j.cej.2021.132754

[4] Wang, H., Yu, L. Q., Chen, S. N., Liu, M., Fan, N. S., Huang, B. C. & Jin, R. C. (2022) Coagulation enhanced high-rate contact-stabilization process for pretreatment of municipal wastewater: Simultaneous organic capture and phosphorus removal, *Separation and Purification Technology, 298*, 121669, https://doi.org/10.1016/j.seppur.2022.121669

[5] Alibardi, L., Vale, P. & Fernández, Y. B. (2021) Full-scale trials to achieve low total phosphorus in effluents from sewage treatment works, *Journal of Water Process Engineering, 40,* 101981, https://doi.org/10.1016/j.jwpe.2021.101981

[6] Zou, H., Wang, T., Wang, Z. L. & Wang, Z. (2023) Continuing large-scale global trade and illegal trade of highly hazardous chemicals, *Nature Sustainability, 6(11),* 1394-1405, https://doi.org/10.1038/s41893-023-01158-w

[7] Etale, A., Onyianta, A. J., Turner, S. R. & Eichhorn, S. J. (2023) Cellulose: a review of water interactions, applications in composites, and water treatment, *Chemical reviews, 123(5),* 2016-2048, https://doi.org/10.1021/acs.chemrev.2c00477

[8] Salim, N. A. A., Fulazzaky, M. A., Puteh, M. H., Khamidun, M. H., Yusoff, A. R. M., Abdullah, N. H. & Nuid, M. (2021) Adsorption of phosphate from aqueous solution onto iron-coated waste mussel shell: Physicochemical characteristics, kinetic, and isotherm studies, *Biointerface Res. Appl. Chem, 11,* 12831-12842, https://doi.org/10.33263/BRIAC115.1283112842

[9] Wang, B., Tang, X., Deng, J., Gan, Y., Li, X., Zhang, F. & Lu, Y. (2023) Application of 13CH4 double model online analysis method based on Fourier Transform Infrared Spectroscopy in energy exploration, *Vibrational Spectroscopy, 129,* 103621, https://doi.org/10.1016/j.vibspec.2023.103621

[10] Salim, N. A. A., Fulazzaky, M. A., Puteh, M. H., Khamidun, M. H., Yusoff, A. R. M., Abdullah, N. H. & Nuid, M. (2021) Adsorption of phosphate from aqueous solution onto iron-coated waste mussel shell: Physicochemical characteristics, kinetic, and isotherm studies, *Biointerface Res. Appl. Chem, 11,* 12831-12842, https://doi.org/10.33263/BRIAC115.1283112842

[11] Park, J. H., Choi, A. Y., Lee, S. L., Lee, J. H., Rho, J. S., Kim, S. H. & Seo, D. C. (2022) Removal of phosphates using eggshells and calcined eggshells in high phosphate solutions, *Applied Biological Chemistry, 65(1),* 75, https://doi.org/10.1186/s13765-022-00744-4

[12] Wang, H., Lin, N., Yuan, S., Liu, Z., Yu, Y., Zeng, Q. & Wu, Y. (2023) Numerical simulation on hydrodynamic lubrication performance of bionic multi-scale composite textures inspired by surface patterns of subcrenata and clam shells, *Tribology International, 181,* 108335, https://doi.org/10.1016/j.triboint.2023.108335

[13] Zhou, Z., Xu, Q., Wu, Z., Fang, X., Zhong, Q., Yang, J. & Li, Q. (2023) Preparation and characterization of clay-oyster shell composite adsorption material and its application in phosphorus removal from wastewater, *Sustainable Chemistry and Pharmacy, 32,* 101023, https://doi.org/10.1016/j.scp.2023.101023

[14] Uzun, O., Gokalp, Z., Irik, H. A., Varol, I. S. & Kanarya, F. O. (2021) Zeolite and pumice-amended mixtures to improve phosphorus removal efficiency of substrate materials from wastewaters, *Journal of Cleaner Production, 317,* 128444, https://doi.org/10.1016/j.jclepro.2021.128444

[15] Odeh, M., Doscher, C. & Cochrane, T. A. (2022) Removal of zinc from surface runoff by using recycled mussel shell waste as treatment media, with and without heat treatment, *Environmental Technology & Innovation, 28,* 102814, https://doi.org/10.1016/j.eti.2022.102814

[16] Salim, N. A. A., Abdullah, N. H., Khairuddin, M. R., Arman, M. A. B. Z. R., Khamidun, M. H., Fulazzaky, M. A. & Puteh, M. H. (2018) Adsorption of phosphate from aqueous solutions using waste mussel shell, *In MATEC Web of Conferences*, *250,* 06013, https://doi.org/10.1051/matecconf/201825006013

[17] Sulaiman, R., Azeman, N. H., Mokhtar, M. H. H., Mobarak, N. N., Bakar, M. H. A. & Bakar, A. A. A. (2024) Hybrid ensemble-based machine learning model for predicting phosphorus concentrations in hydroponic solution, *Spectrochimica Acta Part A: Molecular and Biomolecular Spectroscopy, 304*, 123327, https://doi.org/10.1016/j.saa.2023.123327

[18] Nguyen, T. A. H., Ngo, H. H., Guo, W. S., Nguyen, T. T., Vu, N. D., Soda, S. & Cao, T. H. (2020) White hard clam (Meretrix lyrata) shells as novel filter media to augment the phosphorus removal from wastewater, *Science of the Total Environment, 741,* 140483, https://doi.org/10.1016/j.scitotenv.2020.140483

[19] Liu, X., Wang, Y., Smith, R. L., Fu, J. & Qi, X. (2021) High-capacity structured MgO-Co adsorbent for removal of phosphorus from aqueous solutions, *Chemical Engineering Journal*, *426,* 131381, https://doi.org/10.1016/j.cej.2021.131381

[20] Anwer, S. S. (2023) Direct analysis of algae for determination of major and minor elements using energy dispersive x-ray fluorescence (EDXRF), *Kuwait Journal of Science, 50(4),* 697-702, https://doi.org/10.1016/j.kjs.2023.04.012

[21] Cao, J., Zhao, W., Wang, S., Xu, R., Hao, L. & Sun, W. (2023) Effects of calcium on phosphorus recovery from wastewater by vivianite crystallization: Interaction and mechanism analysis, *Journal of Environmental Chemical Engineering*, *11(5),* 110506, https://doi.org/10.1016/j.jece.2023.110506

[22] Khan, M. K., Abdulhameed, A. S., Alshahrani, H. & Algburi, S. (2024) Chitosan/functionalized fruit stones as a highly efficient adsorbent biomaterial for adsorption of brilliant green dye: Comprehensive characterization and statistical optimization, *International Journal of Biological Macromolecules*, *263,* 130465, https://doi.org/10.1016/j.ijbiomac.2024.130465

[23] Shen, J., Huang, G., An, C., Xin, X., Huang, C. & Rosendahl, S. (2018) Removal of Tetrabromobisphenol A by adsorption on pinecone-derived activated charcoals: Synchrotron FTIR, kinetics and surface functionality analyses, *Bioresource technology*, *247,* 812-820, https://doi.org/10.1016/j.biortech.2017.09.177

[24] Pazo-Cepeda, M. V., Nastasiienko, N. S., Kulik, T. V., Palianytsia, B. B., Alonso, E. & Aspromonte, S. G. (2023) Adsorption and thermal transformation of lignin model compound (ferulic acid) over HY zeolite surface studied by temperature programmed desorption mass-spectrometry, FTIR and UV–Vis spectroscopy, *Microporous and Mesoporous Materials*, *348,* 112394, https://doi.org/10.1016/j.micromeso.2022.112394

[25] Flórez, E., Jimenez-Orozco, C. & Acelas, N. 2024 Unravelling the influence of surface functional groups and surface charge on heavy metal adsorption onto carbonaceous materials: An in-depth DFT study, *Materials Today Communications, 39,* 108647, https://doi.org/10.1016/j.mtcomm.2024.108647

[26] Fumoto, E., Sato, S., Kawamata, Y., Koyama, Y., Yoshikawa, T., Nakasaka, Y. & Masuda, T. (2022) Determination of carbonyl functional groups in lignin-derived fraction using infrared spectroscopy, *Fuel*, *318,* 123530, https://doi.org/10.1016/j.fuel.2022.123530

[27] Pellenz, L., de Oliveira, C. R. S., da Silva Júnior, A. H., da Silva, L. J. S., da Silva, L., de Souza, A. A. U. & da Silva, A. (2023) A comprehensive guide for characterization of adsorbent materials, *Separation and Purification Technology, 305,* 122435, https://doi.org/10.1016/j.seppur.2022.122435

[28] Zheng, X., Pan, C., Zheng, S. & Guo, Y. (2024) Functionalized magnetic chitosan-based adsorbent for efficient tetracycline removal: Deep investigation of adsorption behaviors and mechanisms, *Separation and Purification Technology, 335,* 126212, https://doi.org/10.1016/j.seppur.2023.126212

[29] Martínez-Cano, A., Mendoza-Báez, R., Zenteno-Mateo, B., Rodríguez-Mora, J. I., Agustín-Serrano, R. & Morales, M. A. (2022) Study by DFT of the functionalization of amylose/amylopectin with glycerin monoacetate: Characterization by FTIR, electronic and adsorption properties, *Journal of Molecular Structure, 1269,* 133761, https://doi.org/10.1016/j.molstruc.2022.133761

[30] Xu, Z., Huang, W., Wang, S., Song, H., Xu, J., Mailhot, G. & Li, Z. (2023) Co-adsorption characteristics of antibiotics with different functional groups and cadmium combined contamination on activated carbon, *Journal of Environmental Chemical Engineering*, *11(3),* 110070, https://doi.org/10.1016/j.jece.2023.110070

[31] Shaikh, H. Y., Niazi, S. K., Bepari, A., Assiri, R. A., Rudrappa, M., Chavhan, M. S., & Agadi, S. N. (2023) Phytochemical screening, GCMS profiling, in vitro antioxidant, in vivo acute toxicity, and hepatoprotective activity of Cleome simplicifolia bioactive metabolites against paracetamol-intoxicated wister albino rats, *Applied Sciences*, *14(1),* 46, https://doi.org/10.3390/app14010046

[32] Ghoreishian, S. M., Raju, G. S. R., Pavitra, E., Kwak, C. H., Han, Y. K. & Huh, Y. S. (2019) Ultrasound-assisted heterogeneous degradation of tetracycline over flower-like rGO/CdWO4 hierarchical structures as robust solar-light-responsive photocatalysts: Optimization, kinetics, and mechanism, *Applied Surface Science, 489,* 110-122. https://doi.org/10.1016/j.apsusc.2019.05.299

[33] Hashmi, A. W., Mali, H. S., Meena, A., Saxena, K. K., Ahmad, S., Agrawal, M. K. & Khan, M. I. (2023) A comprehensive review on surface post-treatments for freeform surfaces of bio-implants, *Journal of Materials Research and Technology, 23,* 4866-4908, https://doi.org/10.1016/j.jmrt.2023.02.007

[34] Ezzati, R., Azizi, M. & Ezzati, S. (2024) A theoretical approach for evaluating the contributions of pseudo-first order and pseudo-second-order kinetics models in the Langmuir rate equation, *Vacuum, 222*, 113018, https://doi.org/10.1016/j.vacuum.2024.113018

[35] Ye, T., Min, X., Jiang, X., Sun, M. & Li, X. (2022) Adsorption and desorption of coal gangue toward available phosphorus through calcium-modification with different pH, *Minerals*, *12(7),* 801, https://doi.org/10.3390/min12070801

[36] Revellame, E. D., Fortela, D. L., Sharp, W., Hernandez, R. & Zappi, M. E. (2020) Adsorption kinetic modeling using pseudo-first order and pseudo-second order rate laws: A review, *Cleaner Engineering and Technology, 1,* 100032, https://doi.org/10.1016/j.clet.2020.100032